Influence of ion dynamics on the width and shift of isolated He I lines in plasmas

R. Kobilarov,* N. Konjević, and M. V. Popović
Institute of Physics, 11001 Belgrade, P.O. Box 57, Yugoslavia
(Received 19 April 1989)

We report measured Stark widths and shifts of the neutral helium lines 3889 and 5876 Å in hydrogen-helium, pure helium, and argon-helium plasmas. A pulsed low-pressure arc is used as a plasma source. Electron densities of $(2-10)\times10^{16}$ cm^{-3} are measured by laser interferometry, electron temperatures in the range from 31 000 to 42 000 K are determined from the intensity ratio of O II impurity lines, and the gas temperature is determined from the Doppler component of the O II line profile. Experimental Stark widths and shifts are compared with theoretical results obtained from three sets of semiclassical calculations of Stark-broadening parameters using quasistatic and ion-dynamic treatment of the ions. Inclusion of ion dynamics in the calculation of widths and shifts considerably improves the agreement between theory and experiments. The results of the comparison show a constant systematic discrepancy between three semiclassical calculations and the experiment. These results suggest the possibility of plasma-electron-density diagnostics with a precision in the range 3–5 %.

I. INTRODUCTION

The influence of ion dynamics on the shape and shift of Stark-broadened He I lines has been the subject of numerous experimental and theoretical studies, most of them primarily related to the lines with forbidden components. However, only three papers[1–3] deal with experimental investigations of Stark-broadening parameters of isolated He I lines trying to assess the importance of ion motion to the linewidth and shift. In the first experimental attempt, Morris and Cooper[1] studied shifts of three isolated He I lines in the plasma of a helium jet, where they detected only small deviations from quasistatic behavior. In a detailed study of the line shapes and shifts of 12 He I lines in a wall-stabilized helium arc plasma, Kelleher[2] has found the experimental widths and shifts to be "reasonably consistent with calculations based on the unified theory[4] for ion perturbers." In both these papers[1,2] the dependence of ion dynamics on the helium-atom–perturbing-ion reduced mass was not investigated; therefore, one could only test the validity of the theory through the consistency with the experiment.

In another experiment,[3] the widths and shifts of the 3889- and 5876-Å He I lines were measured in a plasma dominated by proton ion perturbers where one has the largest ion motion effect. Although some preliminary results were reported, quantitative conclusions about the importance of ion dynamics in the linewidth and shift evaluation were not drawn. This was due to the lack of a reliable method for line self-absorption testing and correction in a linear, helium pulsed plasma discharge. This correction is very important in line-shape measurements, e.g., see Ref. 5.

Here we report results of Stark-width and -shift measurements of the He I 3889- and 5876-Å lines in a pulsed plasma source filled with a hydrogen-helium, pure helium, or argon-helium mixture. In this way we could study the broadening and shift of these two He I lines for different emitter–perturbing-ion reduced-mass combinations. To perform this study we applied a new technique to check, and if necessary to correct, for self-absorption of the He I lines in our pulsed low-pressure discharge. The experimental results for these lines are compared with theoretical results obtained using static- and dynamic-ion approximations. The results of this comparison will be used to test the applicability of unified theory[4] in cases when ion motion is important. Simultaneously, several theoretical calculations of He I line Stark widths and shifts will be tested. This is of importance for further development of the theory and for high-precision plasma diagnostics.

II. THEORY

A. Widths

Quasistatic treatment of ions. The full width at half maximum (FWHM) of He I lines, $w_{\rm stat}$, at electron density N_e is calculated from the following equation:[6]

$$w_{\rm stat}=2w_e(1+g\alpha_N)N_e\times10^{-16}\ , \tag{1}$$

where

$$g=1.75(1-0.75R)\ , \tag{2}$$

$$R=\rho_0/\rho_D=(N_e^{1/3})^{1/2}/T_e\ , \tag{3}$$

and

$$\alpha_N=\alpha N_e^{1/4}\times10^{-4}\ . \tag{4}$$

In the above equations w_e and α are the electron-impact half-half-width and ion-broadening parameters, respectively, at $N_e=1\times10^{16}$ cm^{-3}, ρ_0 is the mean inter-ion distance, and ρ_D is the Debye length.

Dynamic treatment of ions. Here, we follow the unified adiabatic theory, independently developed by Griem[6] and by Barnard, Cooper, and Smith (BCS).[4] If strong collisions do not overlap in time, the theory is valid for the whole range of ion broadening, from quasistatic to impact broadening. The relative importance of dynamical ion broadening is contained in the parameter

$$\sigma=\omega_e\rho_0/\langle v_{\rm rel}\rangle ,$$

where

$$\rho_0=(\tfrac{4}{3}\pi N_e)^{-1/3} ,$$
$$\langle v_{\rm rel}\rangle=\left[\frac{8kT_g}{\pi\mu}\right]^{1/2} , \tag{5}$$
$$\omega_e=w_e\frac{2\pi c}{\lambda^2}\times 10^8 .$$

Here $\langle v_{\rm rel}\rangle$ is the mean relative velocity of the radiator and the ion perturber, which have a reduced mass μ_i; ω_e is the electron-impact half-half-width expressed in frequency units. w_e and λ are in angstroms. Equation (5) may also be written[2]

$$\sigma=\frac{0.0806w_e}{\lambda^2}N_e^{2/3}\sqrt{\mu/T_g} , \tag{6}$$

where w_e is the electron half-half-width in angstroms at $N_e=10^{16}$ cm^{-3} and μ is the atom-ion perturber reduced mass in amu. The condition of validity for the ion-dynamics correction is expressed by

$$\beta=\alpha_N^{1/3}\sigma<1 . \tag{7}$$

The physical meaning of this condition is that all strong electron and ion collisions are separated in time, which was satisfied for our experimental conditions.

From the results of BCS,[4] Kelleher[2] derived a simple parametric expression for the evaluation of the total half-width $w_{\rm dyn}$ for dynamic ions of isolated lines when ion dynamics contributes to the linewidth,

$$w_{\rm dyn}=2w_e(1+g\alpha_N W_j)N_e\times 10^{-16} , \tag{8}$$

where

$$W_j=\begin{cases}\dfrac{1.36}{g}\beta^{-1/3}, & \beta<\left[\dfrac{1.36}{g}\right]^3\\ 1, & \beta\geq\left[\dfrac{1.36}{g}\right]^3 .\end{cases} \tag{8'}$$

From the comparison of Eqs. (1) and (8) it follows that $w_{\rm dyn}=w_{\rm stat}$ when $W_j=1$.

B. Shifts

Quasistatic treatment of ions. One can calculate the shift at the peak of the line $d_{\rm stat}$ from[6]

$$d_{\rm stat}=[d_e\pm 2.00\alpha_N(1-0.75R)w_e]N_e\times 10^{-16}$$

or (9)

$$d_{\rm stat}=(d_e\pm 2.00\alpha_N g_1 w_e)N_e\times 10^{-16} ,$$

where $g_1=g/1.75$ and d_e is the electron-impact shift at $N_e=10^{16}$ cm^{-3}.

The shift at the half-width of the line is given by[2]

$$d_{{\rm stat}_{1/2}}=(d_e\pm 3.2\alpha_N g_1 w_e)N_e\times 10^{-16} . \tag{10}$$

The signs of the ion quadratic contribution to the width in Eqs. (9) and (10) are the same as that of d_e, the electron shift. That is, for helium lines the sign is always such that it increases the magnitude of the shift.

Dynamic treatment of ions. Analogous to Eq. (8), we derived for widths from the results of BCS (Ref. 4) expressions for evaluation of shifts at the peak of the line

$$d_{\rm dyn}=(d_e\pm 2.00\alpha_N g_1 D_j w_e)N_e\times 10^{-16} , \tag{11}$$

and at the half-width of the line

$$d_{{\rm dyn}_{1/2}}=(d_e\pm 3.20\alpha_N g_1 D_j w_e)N_e\times 10^{-16} , \tag{12}$$

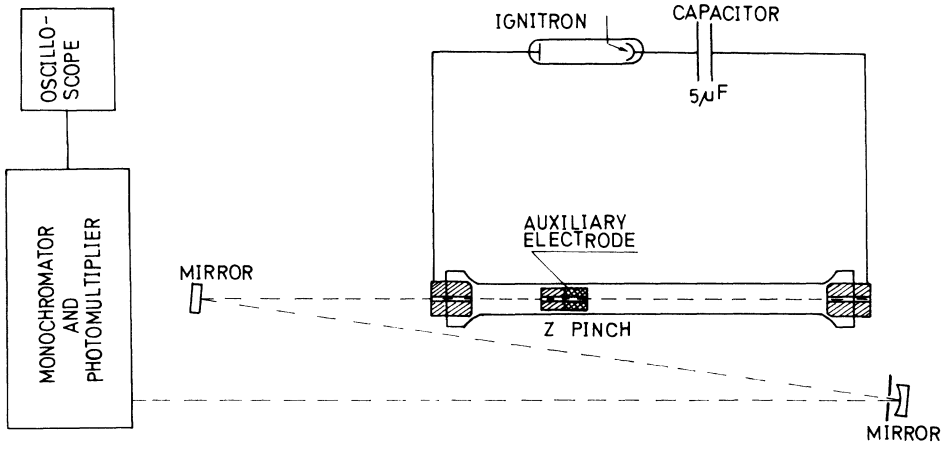

FIG. 1. Schematic diagram of the experimental setup.

where

$$D_j = \begin{cases} \dfrac{2.35\beta^{-1/3} - 3\alpha_N^{1/3} R}{2g_1}, & \beta < 1 \\ 1, & \beta \geq 1 \ . \end{cases} \tag{12'}$$

For $D_j = 1$, $d_{\text{dyn}} = d_{\text{stat}}$ or $d_{\text{stat}_{1/2}} = d_{\text{dyn}_{1/2}}$.

There are certain restrictions on the applicability of Eqs. (1) and (9)–(11) and they are[6]

$$8.99 \times 10^{-2} N_e^{1/6} T^{-1/2} \leq 0.8 \ ,$$

$$0.05 < \alpha_N < 0.5 \ .$$

For large values of α_N, the forbidden component begins to overlap significantly and the linear Stark effect becomes important. Other considerations, such as Debye shielding affecting the line shapes, widths, and shifts are covered in Ref. 6.

For the evaluation of He I Stark widths and shifts from Eqs. (1), (8), (10), and (12) we used w_e, d_e, and α at $N_e = 10^{16}$ cm^{-3} from Benett and Griem[6,7] and Bassalo *et al.*[8] Dimitrijević and Sahal-Bréchot[9] reported only He I electron-impact half-half-widths and shifts which, as the authors[9] suggested, we used with their w_e and d_e values α from Ref. 6.

III. EXPERIMENT

A. Plasma source and experimental procedure

A low-pressure pulsed arc is used as a plasma source (see Fig. 1). It consists of a low inductance discharge capacitor having a peak voltage rating of 25 kV and capacitance of 5 μF. The pulsed arc is fired at 15 kV by an ignitron and the ringing frequency of the whole circuit, including discharge vessel, is 12 μs. The discharge tube is made of Pyrex glass with 13.5 mm internal diameter. The distance between the end electrodes is 28 cm. For the measurements of the optical depth of spectral lines, an additional aluminum electrode with a thin surrounding sleeve of iron is located inside the discharge tube. The iron sleeve is the electrode which can be moved from the outside by means of a magnet. When observing spectra the central hole in this movable electrode is blocked. In this way it is possible to vary the plasma length and, accordingly, the absorption conditions of the plasma layer under investigation without changing the electrical impedance of the circuit. This technique has been used recently by Radtke and Günter[10] to study the Balmer spectrum of hydrogen in the plasma of a flashlamp.

Holes of 1.8 mm diameter are located at the center of all three electrodes to facilitate optical alignment and to perform laser interferometric measurements of the electron density. During the experiment a continuous flow of pure He, or He:H_2 (40:60 mol %) or He:Ar (30:70 mol %) mixtures is maintained at a pressure of 133 Pa (1 torr).

The light from the pulsed arc is observed end-on on a shot-to-shot basis with a 1-m monochromator (inverse linear dispersion 4.2 Å/mm) equipped with photomultiplier tube. This instrument, with 12-μm slits, has a measured instrumental half-width of 0.06 Å. The discharge is imaged onto the entrance slit of the monochromator by means of a concave mirror, see Fig. 1. The diaphragm placed in front of the concave mirror ensures that light comes only from the central 1.5 mm of the plasma about the arc axis. The contribution of instrumental, Doppler, and van der Waals broadening to the He I line-shape measurements for our experimental conditions is found to be negligible.

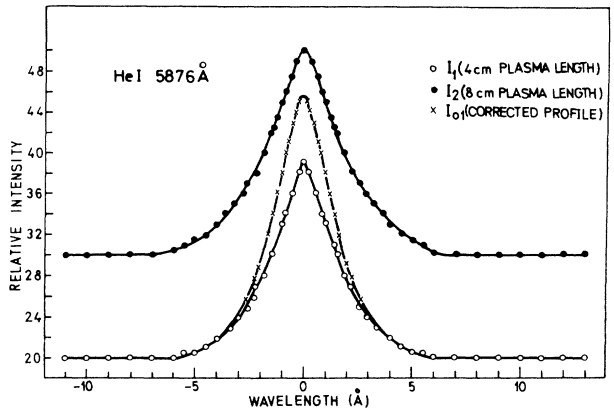

FIG. 2. Experimental profiles of the He I 5876-Å line recorded with two plasma lengths at $N_e = 9.8 \times 10^{16}$ cm^{-3} (upper profile) and $T_e = 42\,000$ K and the derived profile for the optically thin case.

Our main concern with the He I line-shape measurements was the possible distortion arising from self-absorption. In order to determine the optical thickness of the investigated lines we recorded line profiles from two plasma lengths by positioning the movable electrode. From these recordings we determined $k_\lambda l$ where k_λ is the

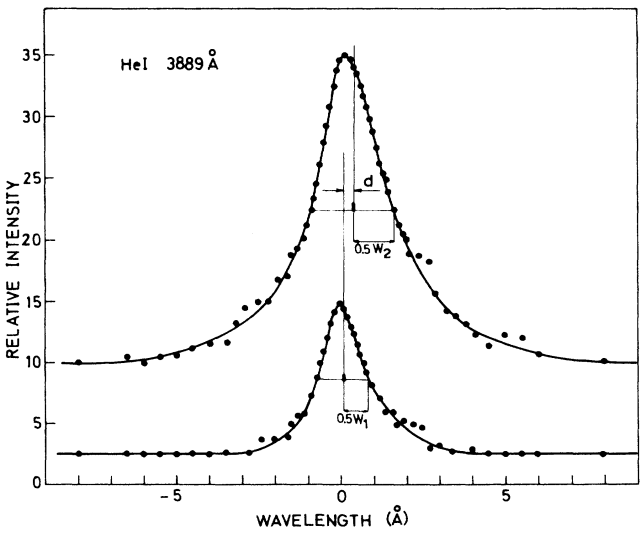

FIG. 3. Two experimental profiles of the He I 3889-Å line obtained at the maximum electron density of 9.8×10^{16} cm^{-3} (upper profile) and at 6.1×10^{16} cm^{-3}; w is the half-width and d is the shift at the half-width.

TABLE I. Ratios of measured w_m and calculated widths using static- w_{stat} and dynamic-ion approximation w_{dyn}. Data for the theoretical calculations are taken from Benett and Griem (BG) (Refs. 6 and 7), Bassalo *et al.* (BCW) (Ref. 8), and Dimitrijević and Sahal-Bréchot (DSB) (Ref. 9); μ is the helium-atom– (emitter) perturbing-ion reduced mass, for the helium-hydrogen mixture, equal to 0.80; $\bar{x}$ is the average value.

λ (Å)	μ	$N_e\times10^{16}$ (cm^{-3})	T_e (K)	T_g (K)	w_m (Å)	w_m/w_{stat} BG	BCW	DSB	w_m/w_{dyn} BG	BCW	DSB
3889	0.80	9.80±0.50	42 000	42 000	2.50±0.15	0.94	1.10	1.16	0.87	1.01	1.06
		6.10±0.50	36 000	36 000	1.51±0.12	0.92	1.08	1.14	0.85	0.97	1.04
	2.00	3.50±0.25	35 500	31 000	0.87±0.08	0.94	1.10	1.17	0.88	1.01	1.08
		1.90±0.25	32 000	27 000	0.46±0.05	0.93	1.08	1.16	0.86	0.98	1.06
	3.64	8.50±0.50	35 000	35 000	1.98±0.15	0.86	1.00	1.07	0.84	0.96	1.03
		5.40±0.50	31 000	31 000	1.24±0.10	0.86	1.00	1.07	0.83	0.95	1.02
								$\bar{x}$			
						0.91	1.06	1.13	0.85	0.98	1.05
5876	0.80	9.80±0.50	42 000	42 000	3.95±0.20	1.00	1.36	1.20	0.91	1.19	1.09
		6.10±0.50	36 000	36 000	2.45±0.15	1.01	1.37	1.21	0.91	1.19	1.08
	3.64	8.50±0.50	35 000	35 000	3.18±0.18	0.93	1.26	1.12	0.89	1.17	1.06
		5.40±0.50	31 000	31 000	2.00±0.15	0.93	1.25	1.12	0.88	1.15	1.05
								$\bar{x}$			
						0.97	1.31	1.16	0.90	1.17	1.07

spectral line absorption coefficient and l is the plasma length along the direction of observation. Since $k_\lambda l$ was not large ($k_\lambda l < 0.31$ for the most self-absorbed analyzed profile) it was possible to recover the line profile (see the example in Fig. 2) for the optically thin case (see, e.g., Ref. 11). The only exception was the strong 5876-Å line in pure helium whose profile was so distorted by self-absorption that the optically thin profile could not be recovered. Corrections for fine-structure splitting were found to be negligible under our conditions (see Fig. 1 in Ref. 2).

For line-shift measurements we used the plasma radiation at the late times of plasma decay as a source of the less-shifted line profile.[12] Thus to measure the line shift it is necessary to analyze oscilloscope traces obtained from the photomultiplier-monochromator system at various wavelengths and at various times of the decay. An example of these measurements is in Fig. 3, where two experimental profiles of He I 5876 Å at electron density $N_e=9.8\times10^{16}$ cm^{-3} and 10 μs later at $N_e=6.1\times10^{16}$ cm^{-3} are given. From Fig. 3 it is possible to determine the line shift, and in the same way all reported measurements are performed. Here one should note that the reported shifts are measured at the half-width of both line

TABLE II. Same as for Table I but for the shifts.

λ (Å)	μ	$N_e\times10^{16}$ (cm^{-3})	T_e (K)	T_g (K)	d_m (Å)	d_m/d_{stat} BG	BCW	DSB	d_m/d_{dyn} BG	BCW	DSB
3889	0.80	9.80±0.50	42 000	42 000	0.30(0)±0.02(5)	1.20	1.60	1.42	0.83	0.99	0.91
		6.10±0.50	36 000	36 000							
	2.00	3.50±0.25	35 500	31 000	0.11(0)±0.01(5)	1.10	1.47	1.21	0.77	0.92	0.83
		1.90±0.25	32 000	27 000							
	3.64	8.50±0.50	35 000	35 000	0.19(0)±0.01(8)	0.89	1.17	1.00	0.77	0.95	0.84
		5.40±0.50	31 000	31 000							
								$\bar{x}$			
						1.06	1.41	1.21	0.79	0.95	0.86
5876	0.80	9.80±0.50	42 000	42 000	−0.28(0)±0.02(5)	1.63	0.83	2.57	0.72	0.49	0.89
		6.10±0.50	36 000	36 000							
	3.64	8.50±0.50	35 000	35 000	−0.17(0)±0.01(8)	1.26	0.59	1.89	0.76	0.43	0.95
		5.40±0.50	31 000	31 000							
								$\bar{x}$			
						1.44	0.71	2.23	0.74	0.46	0.92

TABLE III. Same as for Table I but for the He I Stark widths taken from the paper by Kelleher (Ref. 2); $\bar{x}$ is the average value, while δ is the standard deviation.

λ (Å)	Transition	w_m/w_{stat} BG	w_m/w_{stat} BCW	w_m/w_{stat} DSB	w_m/w_{dyn} BG	w_m/w_{dyn} BCW	w_m/w_{dyn} DSB
7281	$2^1P^\circ-3^1S$	0.96	1.10	1.26	0.89	1.00	1.14
5016	$2^1S-3^1P^\circ$	1.02	1.08	1.20	0.93	0.98	1.08
6678	$2^1P^\circ-3^1D$	1.13	1.24	1.31	0.98	1.06	1.12
7065	$2^3P^\circ-3^3S$	0.90	1.02	1.15	0.82	0.91	1.03
3889	$2^3S-3^3P^\circ$	0.92	1.07	1.18	0.85	0.97	1.08
5876	$2^3P^\circ-3^3D$	1.01	1.30	1.19	0.92	1.15	1.07
5048	$2^1P^\circ-4^1S$	0.93	1.06	1.26	0.90	1.02	1.21
3965	$2^1S-4^1P^\circ$	0.92	0.99	1.15	0.92	0.99	1.15
4713	$2^3P^\circ-4^3S$	0.93	1.07	1.28	0.89	1.01	1.20
3188	$2^3S-4^3P^\circ$	0.94	1.07	1.23	0.92	1.04	1.19
4121	$2^3P^\circ-5^3S$	0.91	0.92	1.31	0.91	0.92	1.29
2945	$2^3S-5^3P^\circ$	0.90	1.01	1.18	0.90	1.01	1.18
				$\bar{x}$			
		0.96	1.08	1.23	0.90	1.01	1.14
				δ			
		±0.02	±0.03	±0.02	±0.01	±0.02	±0.02
	Experimental conditions: $N_e=1.03\times10^{16}$ cm^{-3}, $T_e=20900$ K, $T_g=15800$ K						

profiles. Furthermore, all fittings of experimental points at the line profile were performed with the aid of a computer.

B. Plasma diagnostics

A helium-neon laser interferometer at 6328 Å with a plane external mirror was used to determine the axial electron density. The electron temperature was determined from the relative intensity of two O II impurity lines at 4366.9 and 4369.3 Å with transition probabilities taken from Ref. 13. The gas temperature is estimated from the Gaussian part of the experimental profile of the O II 4369.3-Å line.

IV. EXPERIMENTAL RESULTS AND DISCUSSION

The experimental results for Stark widths w_m and Stark shifts d_m of the He I lines are given together with estimated errors in Tables I and II, respectively. In these tables the corresponding electron densities, electron temperatures, and gas temperatures are also given. Estimat-

TABLE IV. Same as for Table III but for the He I Stark shifts taken from the paper by Kelleher (Ref. 2).

λ (Å)	Transition	d_m/d_{stat} BG	d_m/d_{stat} BCW	d_m/d_{stat} DSB	d_m/d_{dyn} BG	d_m/d_{dyn} BCW	d_m/d_{dyn} DSB
7281	$2^1P^\circ-3^1S$	1.11	1.19	1.03	0.86	0.90	0.83
5016	$2^1S-3^1P^\circ$	1.03	0.95	1.21	0.70	0.66	0.79
6678	$2^1P^\circ-3^1D$	1.10	1.36	1.24	0.68	0.76	0.75
7065	$2^3P^\circ-3^3S$	1.15	1.22	1.08	0.88	0.92	0.86
3889	$2^3S-3^3P^\circ$	1.22	1.61	1.27	0.79	0.94	0.85
5876	$2^3P^\circ-3^3D$	1.51	0.75	2.69	0.68	0.47	0.90
5048	$2^1P^\circ-4^1S$	1.09	1.18	1.09	0.96	1.02	0.96
3965	$2^1S-4^1P^\circ$	0.84	0.83	1.17	0.84	0.83	1.17
4713	$2^3P^\circ-4^3S$	1.10	1.17	1.05	0.93	0.97	0.90
3188	$2^3S-4^3P^\circ$	1.11	1.17	1.20	0.94	0.96	0.99
4121	$2^3P^\circ-5^3S$	0.99	0.92	1.05	0.99	0.92	0.99
2945	$2^3S-5^3P^\circ$	1.00	1.19	1.24	1.00	1.19	1.24
				$\bar{x}$			
		1.10	1.13	1.28	0.85	0.88	0.94
				δ			
		±0.05	±0.07	±0.13	±0.03	±0.05	±0.04
	Experimental conditions: $N_e=1.03\times10^{16}$ cm^{-3}, $T_e=20900$ K, $T_g=15800$ K						

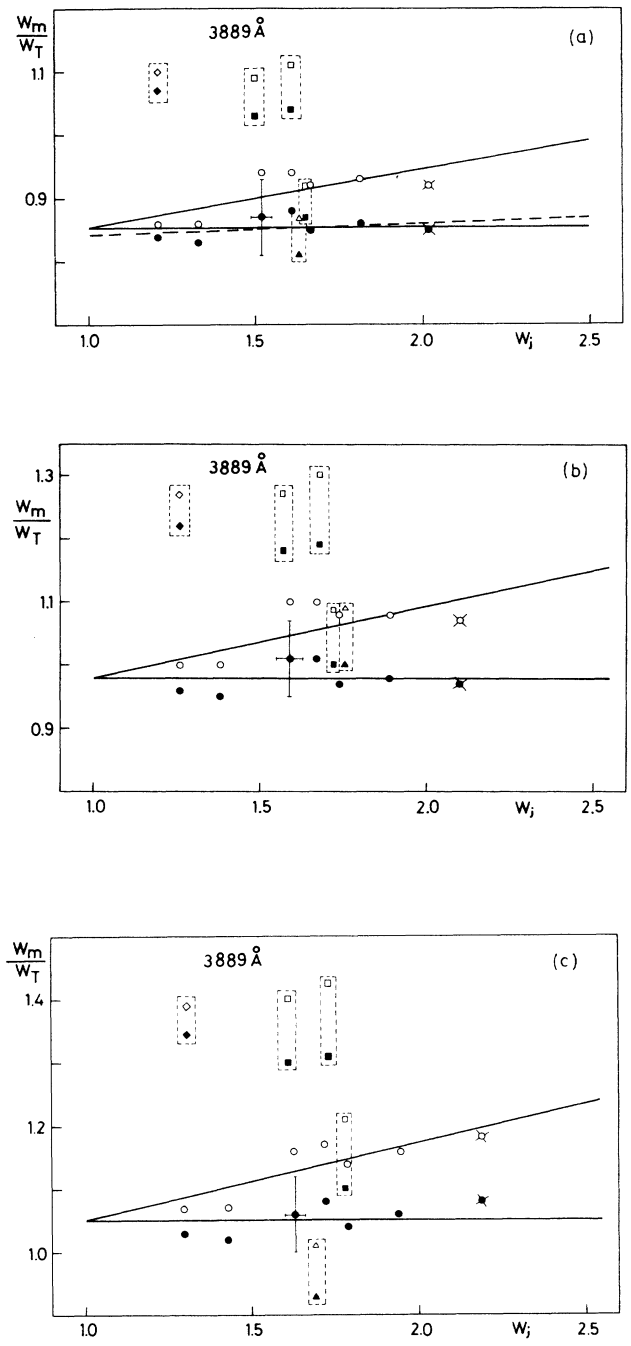

FIG. 4. Ratios of measured w_m over theoretical w_T widths of He I 3889-Å line vs the dynamic-ion broadening parameter W_j of Eq. (8'). Experimental results are compared with theoretical data evaluated from Eq. (1), quasistatic, and Eq. (8), dynamic treatment of ions using electron-impact half-width w_e, and ion-broadenings parameter α: (a) from Benett and Griem (Ref. 6), (b) from Bassalo *et al.* (Ref. 8), and (c) from Dimitrijević and Sahal-Bréchot (Ref. 9); here α is taken from Ref. 6. Ratios w_m/w_T are denoted in the following way. Open symbols denote static ions, closed symbols denote dynamic ions. ⋈, ⋈, Kelleher (Ref. 2); △, ▲, Wulff (Ref. 14); ◇, ◆, Berg *et al.* (Ref. 15); □, ■, Soltwisch and Kusch (Ref. 16); ○, ●, this experiment. The dashed curve in (a) is a best-fit line.

ed errors ranging from 8–12 % for the electron density are derived from uncertainties in the plasma length measurement (by far the largest error) and in the determination of interference fringes. The estimated error in the measurements of the electron temperature T_e is ±8%. This is derived from the uncertainty in the line intensity measurements. The gas temperature T_g is found, within the limits of experimental error of ±15%, equal to electron temperature, i.e., $T_e \approx T_g$. The only exception with $T_e \neq T_g$ is the discharge in pure helium, see Tables I and II.

The experimental results for w_m and d_m in Tables I and II are compared with the theoretical data w_{stat} and $d_{\text{stat}_{1/2}}$ calculated from Eqs. (1) and (10) using the data of Benett and Griem,[6,7] Bassalo *et al.*,[8] and Dimitrijević and Sahal-Bréchot,[9] denoted in Tables I and II as BG, BCW, and DSB, respectively. The experimental data w_m

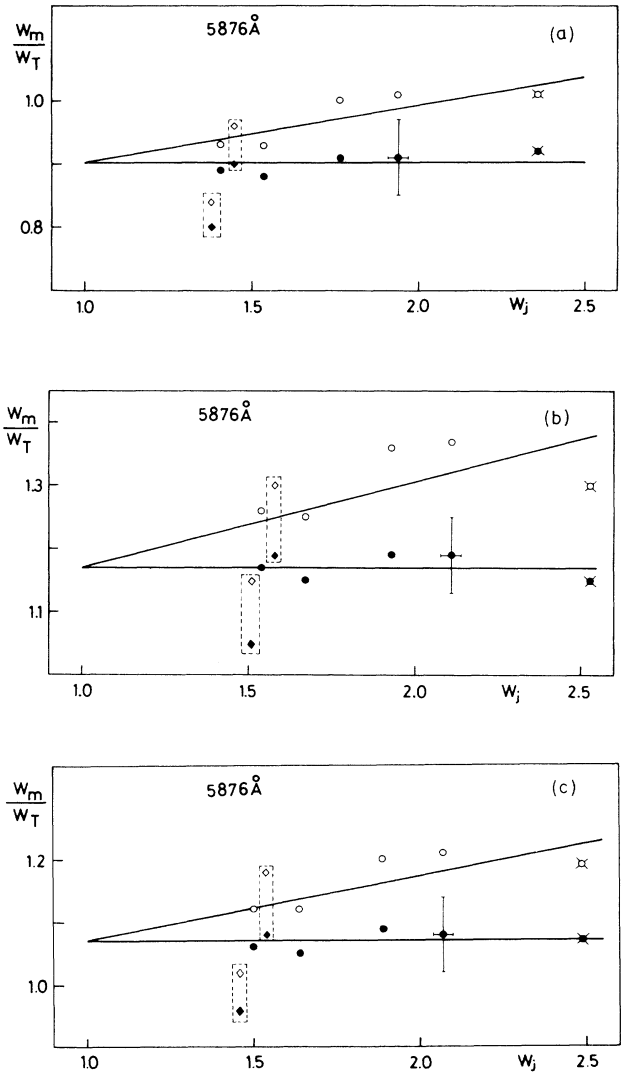

FIG. 5. Same as in Fig. 4 but for the He I 5876-Å line.

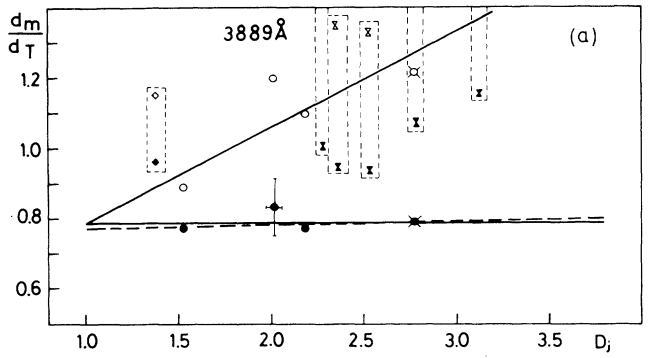

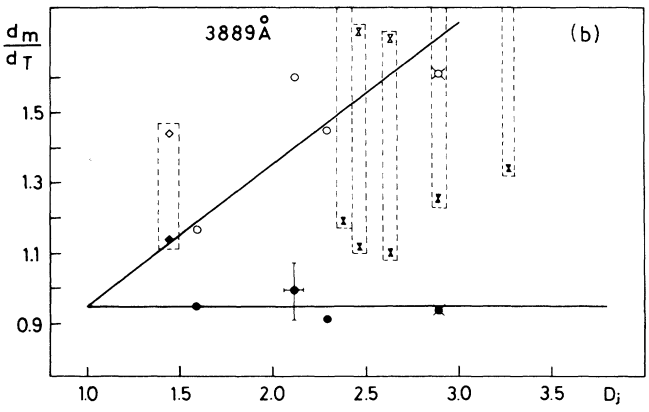

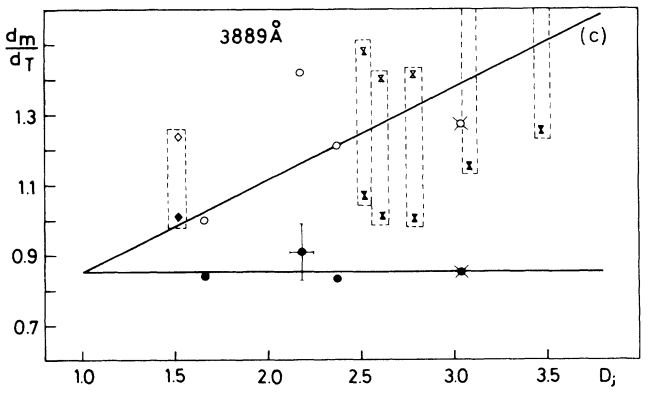

FIG. 6. Ratios of measured d_m over theoretical shifts for the 3889-Å line vs dynamic-ion-broadening parameter D_j of Eq. (12'). Experimental results are compared with theoretical data evaluated from Eq. (10), quasistatic, and from Eq. (12), dynamic, treatment of ions using electron-impact half–half-widths w_e, shifts d_e, and ion-broadening parameter α: (a) from Benett and Griem (Ref. 6), (b) from Bassalo *et al.* (Ref. 8), and (c) from Dimitrijević and Sahal-Bréchot (Ref. 9) (here α is taken from Ref. 6). Ratios d_m/d_T are denoted in the following way. Open symbols denote static ions, closed symbols denote dynamic ions. ⌑,✖,Kelleher (Ref. 2); ◇,◆, Berg *et al.* (Ref. 15); △,▲, Morris and Cooper (Ref. 1); ○,●, this experiment. The dashed curve is a best-fit line.

and d_m are also compared with theoretical results with ion dynamics taken in account, where w_{dyn} and $d_{\text{dyn}_{1/2}}$ are calculated from Eqs. (8) and (12). The required data w_e, d_e, and α are taken from Ref. 6 (BG), Ref. 8 (BCW), and Ref. 9 (DSB). It is important to note here that all theoretically calculated widths and shifts are corrected for the Debye shielding effect in a way described in Ref. 6. Furthermore, in the evaluation of ion-dynamic effects we made an important assumption concerning the type of ions present in the plasma. Namely, due to the large differences in ionization potentials in the hydrogen-helium and in argon-helium mixtures, we assumed that

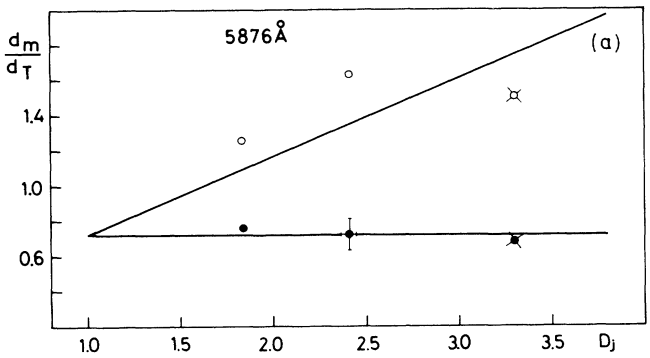

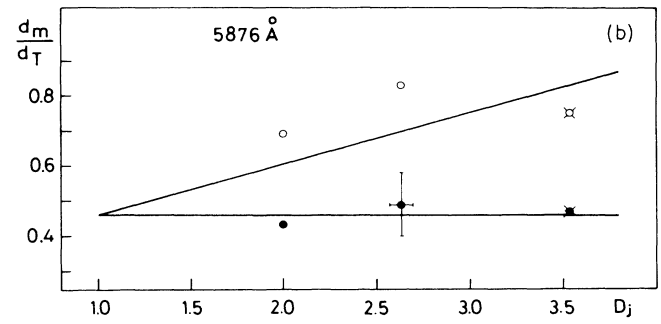

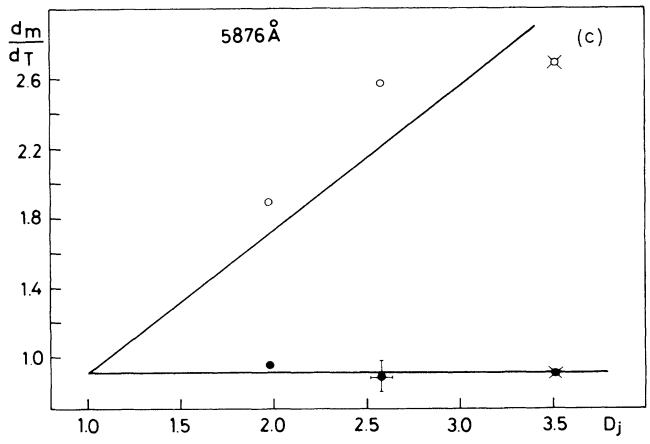

FIG. 7. Same as in Fig. 6 but for the He I 5876-Å line.

TABLE V. Ratios of the measured widths w_m and shifts d_m of He I 3889- and 5876-Å lines to the theoretical results, w_T, derived from Figs. 4–7 for W_j and $D_j = 1$. BG, BCW, and DSB denote ratios with theoretical results using data from Benett and Griem (Refs. 6 and 7), Bassalo *et al.* (Ref. 8), and Dimitrijević and Sahal-Bréchot (Ref. 9), respectively.

	3889 Å		5876 Å	
	Half-width	Shift	Half-width	Shift
BG	0.85±0.03	0.79±0.04	0.90±0.02	0.72±0.04
BCW	0.98±0.03	0.95±0.04	1.17±0.02	0.46±0.03
DSB	1.05±0.03	0.86±0.05	1.07±0.02	0.91±0.04

only H^+ or Ar^+ ions are present in the plasma.

Since we shall also use experimental data from Ref. 2 for comparison, we have calculated the corresponding theoretical widths and shifts in the way described for our data in the preceding paragraph. Ratios of experimental[2] and theoretical results are given in Tables III and IV. Here one should state that all theoretical data marked with BG in Table III are identical with those calculated by Kelleher.[2] This is also the case with the BG theoretical results with the static-ion treatment of shifts in Table IV. In the columns for dynamic-ion treatment under BG, theoretical shifts at the half-width are compared with corresponding shifts reported in Ref. 2.

In order to be able to compare the experimental results measured at different plasma conditions (various N_e, T_e, and T_g) we have plotted in Figs. 4–7 the ratios of measured over theoretical results versus the dynamic-ion broadening parameter W_j from Eq. (8′) and D_j from Eq. (12′) for widths and shifts, respectively. In these figures other precision data,[1,14–16] with estimated uncertainties smaller than ±30% in critical reviews,[17,18] are included also. However, in the analysis of Figs. 4–7 we have used only the recent experiment by Kelleher[2] and our data from Tables I and II. These two sets of data are the most accurate; the estimated total errors in the width and shift measurements are in the range from 15–20 %. Thus data from Refs. 1 and 14–16 placed in rectangles in Figs. 4–6 are not included in the determination of the best-fit straight lines drawn through the experimental points. The curve through the data corrected for ion motion effects (horizontal line) is drawn through the value of the average ratio. This line is very close (within 2%) to the best-fit curve, see Figs. 4(a) and 6(a). This indicates that the correction for ion-dynamic can be properly evaluated using BCS (Ref. 4) in a large range of dynamic-ion broadening parameters. For determining the best-fit line through the ratios of measured and quasistatic theoretical data in Figs. 4–7, we assumed only that this curve started at $W_j = 1$ or $D_j = 1$, where both approximations, quasistatic and dynamic, must give equal theoretical width or shift.

Although the estimated experimental error bars in Figs. 4–7 are very large, the scatter of data from Tables I–IV does not exceed ±3% in the worst case, suggesting that the estimation of accuracies for both experiments may have been too conservative. Furthermore, from Figs. 4–7 one can determine the accuracy of data of three theoretical calculations[6–9] used for the evaluation of Stark widths and shifts and these results are summarized in Table V. The ratios in Table V can be used for two purposes: first, for the further refinement of the theory, because neutral helium has a well-known and reliable set of energy levels which is of crucial importance; second, knowing the ratios in Table V, we can use any of the three theoretical approaches[6–9] in conjunction with one's measurement of widths, and/or shifts, for high-precision plasma diagnostics. On the basis of the experimental scatter in Figs. 4–7 we believe that the plasma electron density, in the electron temperature range 21 000–42 000 K, can be determined from the width and shift of the He I 3889- and 5876-Å lines with a precision of 3–5 %, which is equal to or better than from the H_β line.[19] The estimated uncertainties in Figs. 4–7 are estimated from the spectroscopic and electron density measurements.

V. CONCLUSIONS

In this paper we present results of the measurement of Stark widths and shifts of He I 3889- and 5876-Å lines. Shapes and shifts of these lines were measured in hydrogen-helium, pure helium, and argon-helium plasmas of a pulsed low-pressure arc in the electron-density range of $1.9–9.8\times10^{16}$ cm^{-3} and an electron temperature range of 31 000–42 000 K. In order to obtain He I line profiles for the optically thin case, we have introduced a new technique for the measurement of optical thickness in the plasma of long pulsed arcs.

Experimental results are compared with the data from semiclassical calculations by Benett and Griem,[6,7] Bassalo *et al.*,[8] and Dimitrijević and Sahal-Bréchot,[9] using quasistatic[6] and ion-dynamic[4] approximations. Here we derived a simple analytical expression, similar to the one derived by Kelleher[2] for widths, Eq. (8), which very closely approximates the dynamic-ion contribution to the shift, Eqs. (11) and (12), of the unified theory.[4]

Comparisons of our results and those from Ref. 2 in Figs. 4–7 clearly indicate that the BCS theory[4] correctly describes the dynamic contribution of ions to the Stark width and shift. From Figs. 4–7 we derived ratios of measured to theoretical widths and shifts (see Table V) for three sets of semiclassical calculations.[6–9] Data from Table V can be used as a guide for the further development of the theory and for high-precision plasma diagnostics in the electron temperature range 21 000–42 000 K. We estimate that by measuring widths and/or shifts of He I 3889- and 5876-Å lines and using any of the semi-

classical calculations,[6–9] corrected by the respective values in Table V, one can determine plasma electron density with a precision of ±35%. It is possible that this also represents the absolute accuracy in this temperature and density range, because two independent experiments with completely different diagnostic techniques agree to within this 3–5 % range. However, further confirmation is needed.

---

*Permanent address: Institute of Physics, Faculty of Natural Sciences, 21000 Novi Sad, Yugoslavia.

[1]R. N. Morris and J. Cooper, Can. J. Phys. **51**, 1746 (1973).
[2]D. E. Kelleher, J. Quant. Spectrosc. Radiat. Transfer **25**, 121 (1981).
[3]T. Pittman and N. Konjević, in *Spectral Line Shapes,* edited by F. Rostas (de Gruyter, Berlin, 1985), Vol. 3, p. 79.
[4]J. Barnard, J. Cooper, and E. W. Smith, J. Quant. Spectrosc. Radiat. Transfer **14**, 1025 (1974).
[5]N. Konjević and W. L. Wiese, J. Phys. Chem. Ref. Data **5**, 259 (1976).
[6]H. R. Griem, *Spectral Line Broadening by Plasmas* (Academic, New York, 1974).
[7]S. M. Benett and H. R. Griem, Technical Report No. 71-097, University of Maryland 1971 (unpublished).
[8]J. M. Bassalo, M. Cattani, and V. S. Walder, J. Quant. Spectrosc. Radiat. Transfer **28**, 75 (1982).
[9]M. S. Dimitrijević and S. Sahal-Bréchot, J. Quant. Spectrosc. Radiat. Transfer **31**, 301 (1984).
[10]R. Radtke and K. Günter, Contrib. Plasma Phys. **26**, 143 (1986).
[11]W. L. Wiese, in *Plasma Diagnostic Techniques,* edited by R. M. Huddleston and S. L. Leonard (Academic, New York, 1965).
[12]J. Purić and N. Konjević, Z. Phys. **249**, 440 (1972).
[13]W. L. Wiese, M. W. Smith, and B. M. Glenon, *Atomic Transition Probabilities,* Natl. Bur. Stand. Ref. Data Ser., Natl. Bur. Stand. (U.S.) Circ. No. 4 (U.S. GPO, Washington, D.C., 1966), Vol. I.
[14]H. Wulff, Z. Phys. **150**, 614 (1958).
[15]H. F. Berg, A. W. Ali, R. Lincke, and H. R. Griem, Phys. Rev. **125**, 199 (1962).
[16]H. Soltwisch and H. J. Kusch, Z. Naturforsch. **34A**, 300 (1979).
[17]N. Konjević and J. R. Roberts, J. Phys. Chem. Ref. Data **5**, 209 (1976).
[18]N. Konjević, M. S. Dimitrijević, and W. L. Wiese, J. Phys. Chem. Ref. Data **13**, 619 (1984).
[19]W. L. Wiese, D. E. Kelleher, and D. R. Paquette, Phys. Rev. A **6**, 1132 (1972).